Mechanistic Study of Nano-Particle Fluidization

X. S. Wang[*]   F. Rahman[†]

Martin J Rhodes[‡]

[*]Monash University

[†]Monash University

[‡]Monash University, martin.rhodes@eng.monash.edu.au

MECHANISTIC STUDY OF NANO-PARTICLE FLUIDIZATION

X.S. Wang, F. Rahman, M.J. Rhodes[*]

Department of Chemical Engineering, Monash University,

P.O. Box 36, Clayton 3800, Australia

[†]T: 61-3-9905-3445; F: 61-3-9905-5686; E: martin.rhodes@eng.monash.edu.au

ABSTRACT

Degussa Aerosil R974 powder, with a primary particle size of 12 nm, was fluidized using nitrogen in a cylindrical vessel, 50-mm-id and 900 mm in height. Characteristics of incipient fluidization are analysed in relation to variations in the initial packing conditions. Bed collapse experiments were performed and the results are used for assessing fluidization characteristics of the particles. It was found that nanoparticles exhibit characteristics of both Group A and Group C powders. Various methods for estimating the cohesion forces between nanoparticle aggregates are discussed.

INTRODUCTION

Nanoparticle fluidization has been a topic of increasing research interests over recent years due to its potential applications in reaction engineering, particle formation, processing and coating. Previous studies have shown that nanoparticles may be fluidized in the form of 'light' and 'loose' aggregates, and that the fluidized nanoparticles are 'fluid-like'. Despite some concerted efforts devoted to this topic (e.g., [1] – [4]), our understanding of nanoparticle fluidization is still far from satisfactory. In fact, very little is known about the conditions associated with the start of fluidization of these particles. In addition, although it is commonly perceived that interparticle forces play an important role in determining the characteristics of nano-particle fluidization, there is a lack of quantitative studies of the cohesion forces between nanoparticle aggregates. In this study, the above issues are addressed through a combination of experimental and analytical studies.

EXPERIMENTAL

The fluidized bed used in this study is shown schematically in Fig. 1. The fluidization vessel was a glass tube of 50 mm id and 900 mm in height. High-purity nitrogen was supplied to the bed through a porous distributor plate, 3 mm thick, made from sintered bronze with a nominal pore size of 10 μm. The flow rate of nitrogen was controlled by a needle valve and measured with a rotameter. The particles used

were Aerosil R974 (Degussa) hydrophobic silica. The primary particle size and density were 12 nm and 2200 kg/m^3 respectively, with a bulk density of 30 kg/m^3 and external surface area of 200 m^2/g. The pressure drop through the bed was measured with a digital manometer. Before being vented to the atmosphere, the exhaust gas was filtered using a porous metal filter with 5 μm nominal pore size, and further cleaned by water scrubbing. The pressure drop through the porous metal filter was monitored using a normal water-manometer. The metal filter was cleaned using reversed pulsed flow of nitrogen before each experiment.
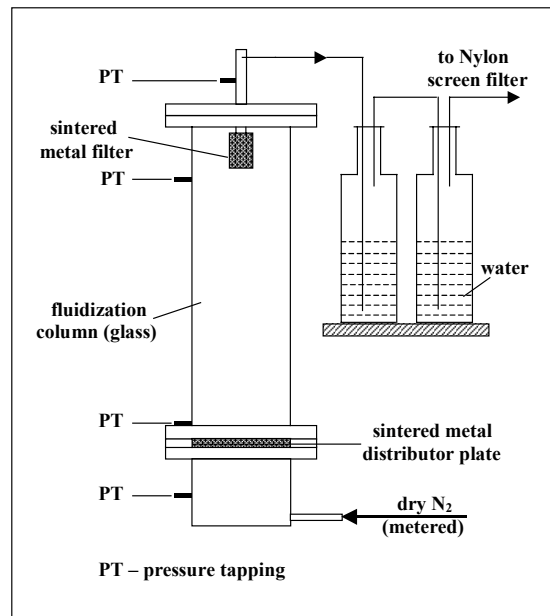
Fig. 1: Schematic diagram of experimental set-up.

RESULTS AND DISCUSSION

Incipient Fluidization of Nanosized Particles
Characteristics of incipient fluidization were investigated by increasing the superficial gas velocity in small steps (e.g., 0.5 mm/s). After each velocity increment, any motion of the particles in the bed was noted and the bed pressure drop and bed expansion ratio were recorded. A typical curve of bed pressure drop as a function of increasing velocity is shown in Fig. 2. When the gas velocity was very low, e.g., below 0.1 cm/s, the pressure drop was low and the motion of particles was negligible. The pressure drop gradually increased with increasing gas velocity, and a point was reached at which the pressure drop approximately balanced the weight of the particles per unit area. As the velocity was further increased, the pressure drop continued to increase until the pressure drop was about 15% above the weight of the particles per unit area. Further increase in gas velocity led to the start of fluidization and evident bed expansion.

The amount of pressure drop above the weight of the particles per unit area has been loosely termed as "overpressure" and "pressure overshoot" in the fluidization

literature. These terms are used interchangeably in this paper for ease of description.
The overpressure was required for overcoming the adhesion between the particles
and the distributor plate, together with any friction between the particles and the
walls. We have observed that the pressure overshoot remained constant (about 1 Pa)
when the static bed height was relatively small (e.g. below 30 mm). As the static bed
height was relatively large (e.g., above 50 mm), an overpressure of up to 3 Pa was
obtained, indicating that the wall friction plays an increasing role in the overall
pressure drop for these conditions.
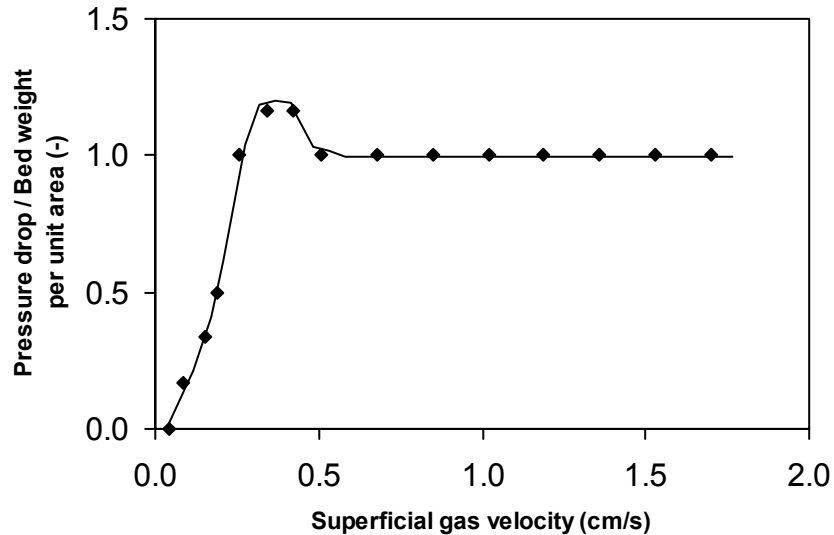
Fig. 2   Variation of bed pressure drop as a function of increasing superficial
gas velocity (even packing; static bed height = 25 mm).

The fluidization behaviour shown in Fig. 2 represents an idealized packed-bed
condition where the particles are fairly uniformly distributed. In this case, the
overpressure enables breaking of the bonding between the particles and the
distributor plate, as well as any interconnected channels and cracks formed for the
lower velocity range. So, soon after the occurrence of fluidization, the pressure drop
decreased to, and remained at, a level which approximately balanced the weight of
the particles per unit area.

In the case of initial uneven packing of particles in the bed, the pressure overshoot
was found to be accompanied by vigorous eruption of particles via local channels.
With increase in gas velocity, the channels were observed to merge and fluidization
was found to first occur near the central region of the bed. The fluidized region then
expanded towards the walls until the whole bed became fluidized. The reason for
delayed fluidization near the walls is that the particles tended to stick around the
corners of the distributor plate. Since only a proportion of the particles participated
at the initial stage of fluidization, we would expect a region where the pressure drop
is smaller than the weight of the particles per unit area. An example of this
behaviour is shown in Fig. 3.
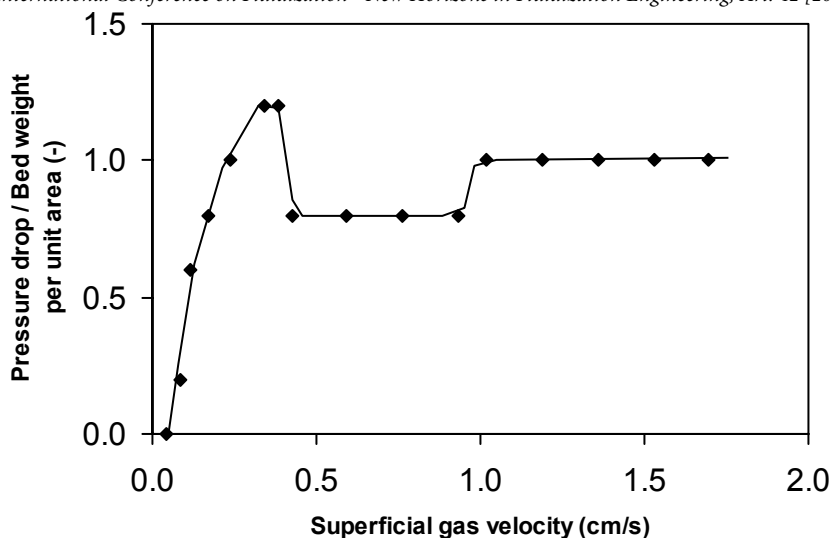
Fig. 3   Variation of bed pressure drop as a function of increasing superficial
gas velocity (uneven packing; static bed height = 17.5 mm).

In cases of strong bonding between the particles and the distributor plate, e.g., after the particles were left in the bed for too long, a relatively high pressure drop was observed even at very low gas velocities (e.g., about 0.5 Pa at a superficial gas velocity of 0.1 cm/s). This is because the gas flow was initially blocked due to tight packing of the particles. These observations suggest that nanoparticles exhibit typical Group C behaviour before fluidization occurs.

The Cohesive Nature of Nano-Particle Fluidization
Due to their sizes, nano-particles would fall in the 'cohesive' category of the Geldart (5) diagram. These particles are usually difficult to fluidize. Yet mounting experimental evidences show that these particles may achieve homogeneous (bubble-less) fluidization with considerable bed expansion, which partly resembles a Group A behaviour. We performed bed collapse experiments in order to determine whether the fluidization behaviour of nanoparticles should be classified as 'cohesive' or Group A. In these experiments the particles were first fully fluidized. The gas supply was then abruptly stopped. The process of particle settling was recorded by a video camera at 25 frames per second. A plot of the variation of bed height with time is shown in Fig. 4. For comparison, a typical bed-collapse curve for Group A particles is also shown in this figure. The head of the bed initially fell at a fairly constant velocity, as particle aggregates were sufficiently separated from each other at this stage. After about 5 s, the inter-aggregate cohesion force started to dominate and the settling process was hindered. The collapse curve obtained consists of two stages: a hindered sedimentation stage and a solid consolidation stage. Unlike Group A powders, no sharp transition between the sedimentation stage and the solid consolidation stage was evident for nanoparticles. In addition, a relatively longer consolidation stage was observed for nanoparticles. The above results point to a typical Group C behaviour for nanoparticles. Geldart *et al*. (6) suggested that the Group C powders might remain in a slightly aerated state for a considerable period, from several minutes to several hours.
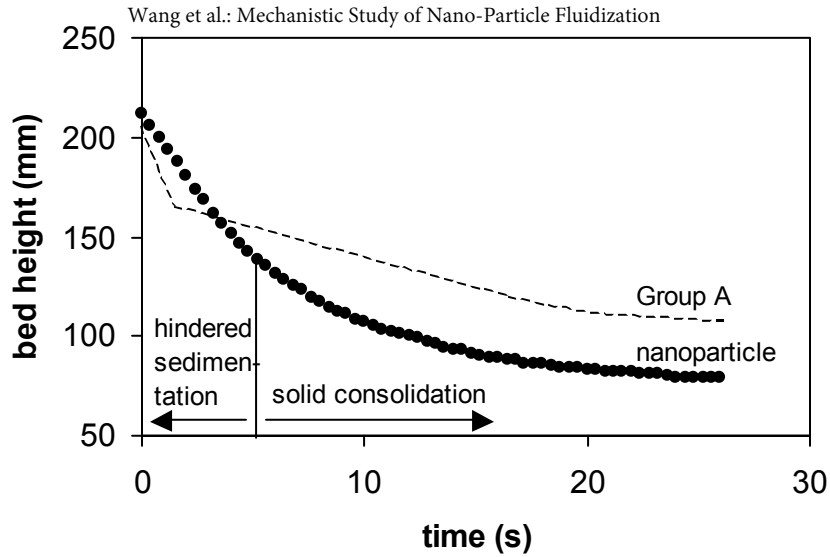
Fig. 4   Example of bed collapse after fluidizing gas was
turned off (static bed height = 75 mm).

Calculation of Inter-Aggregate Cohesion Force
It is now known that nanoparticles are fluidized in the form of loose aggregates. These aggregates differ from normal particles in that their sizes may adjust to operating conditions, e.g., changing gas velocities ($\underline{7}$). Most of the reported sizes for the aggregates are in the 100 to 300 μm range. Wang et al. ($\underline{7}$) found that the sizes of Aerosil R974 particles are about 220 μm surrounding the incipient fluidization conditions. The average void fraction of the aggregates was found to be about 0.99 ($\underline{8}$), which gives a density of about 22 kg/m^3 for the aggregates. In the discussion below, we will assess various methods for calculation of the cohesion forces between the aggregates.

Hamaker's microscopic approach
The van der Waals force between two spherical aggregates may be estimated by Hamaker's microscopic theory ($\underline{9}$ - $\underline{11}$), as expressed in Eq. (1)

$$F = \frac{A_{mi}}{12Z_0^{\,2}} \cdot \frac{d_a d_{asp}}{d_a + d_{asp}} \qquad (1)$$

in which A_{mi} is Hamaker constant, which is 5×10^{-19} J for SiO$_2$ for the microscopic theory ($\underline{12}$), Z_0 is the distance where the van der Waals force is maximum, approximately 4×10^{-10} m, d_a is aggregate diameter, and d_{asp} is the diameter of asperity. In our case, d_a = 220 μm and d_{asp} = 12 nm. The inter-aggregate cohesion force calculated from Eq. (1) is 3.13 nN for our conditions.

Lifshitz's macroscopic theory
Another well-known approach for calculating the attractive force between two spheres is based on Lifshitz's macroscopic theory ($\underline{9}$), as expressed in Eq. (2),

$$F = \frac{h\varpi}{8\pi Z^{\,2}} R[1 + \frac{h\varpi}{8\pi^2 Z^{\,3} H}] \qquad (2)$$

The 12th International Conference on Fluidization - New Horizons in Fluidization Engineering, Art. 42 [2007]

The term $h\varpi$ is a Lifshitz-van der Waals constant, which is related to the Hamaker constant A_{ma} by $h\varpi = (4/3)\pi A_{ma}$. The value of A_{ma} is 8.55×10^{-20} J for SiO_2 particles (12). H in Eq. (2) describes the hardness of the bodies in contact, which is 10^8 N/m^2 for undeformable solids. Parameter R is a geometric mean of the radii of the spheres in contact, defined as R = $(R_1 R_2)/(R_1 + R_2)$, where R_1 and R_2 are radii of the spheres. Rumpf (10) proposed the following modified expression to account for presence of surface asperities

$$F = \frac{h\varpi}{8\pi}[\frac{r}{Z_0^2} + \frac{R}{(r+Z_0)^2}] \qquad\qquad (3)$$

Parameter r in Eq. (3) represents a geometric mean of the radii of asperities, i.e., r = $(r_1 r_2)/(r_1 + r_2)$, where r_1 and r_2 are radii of the asperities. The values of r and R are 3 nm and 55 μm, respectively, in our case, assuming $r_1 = r_2 = 0.5 \times$ (primary particle diameter) and $R_1 = R_2 = 0.5 \times d_a$. These give an inter-aggregate force of 67.2 nN.

Calculation based on measurement of pressure overshoot
Valverde et al. (13) have shown that, provided that the static bed height is small, the tensile yield stress of a cohesive powder (σ) approximately equals the pressure overshoot at incipient fluidization. The tensile stress is related to the cohesion force between the aggregates by the following expression (10, 11),

$$\sigma = \frac{(1-\varepsilon)Fk}{d_a^2 \pi} \qquad\qquad (4)$$

where d_a is aggregate diameter, k is coordination number, i.e., the number of contacts per aggregate, and ε is void fraction around the aggregates. Jaraiz et al. (14) proposed the following cubic equation for calculating the coordination number from the void fraction around the aggregates,

$$k = 17.517 - 41.838\varepsilon + 37.082\varepsilon^2 - 10.815\varepsilon^3 \qquad (5)$$

For a voidage around the aggregates of 0.47, the value of k is found to be about 4.92. For d_a = 220 μm and σ = 1 Pa from our experiments, we find F = 58.3 nN.

Assessment of different approaches
For a particle aggregate to be fluidized, the drag force acting on the aggregate should approximately balance its buoyant weight. It is therefore constructive to compare the cohesion forces in relation to the buoyant weight of a single aggregate (F_g). The value of F_g can be calculated from the following expression:

$$F_g = \frac{1}{6}\pi d_a^3 (\rho_a - \rho_g)g \qquad\qquad (6)$$

where ρ_a and ρ_g are aggregate and gas density, respectively. For ρ_a = 22 kg/m^3 (assuming a void fraction of 0.99 for the aggregate) and ρ_g = 1.22 kg/m^3, we find F_g = 1.14 nN for an aggregate of 220 μm in diameter.

Let's use K to denote the ratio of the inter-aggregate cohesion force to the buoyant weight of a single aggregate, i.e., K = F/F_g. The value of K provides a good indication of the characteristics of fluidization (15). As a rough guide, the value of K should be

below 3 for Group B particles, between 3 and 40 for Group A particles, and above 40 for cohesive particles ([15], [16]). The values of K based on various approaches for calculation of the inter-aggregate forces are given below:

      2.75   - Hamaker's microscopic theory
      58.95 - Lifshitz's macroscopic theory
      51.14 - Calculation based on pressure overshoot

It is interesting to note that the value of K based on Lifshitz's macroscopic theory is comparable with the value based on the measurement of pressure overshoot. These values point to a cohesive behaviour, which is in agreement with the results presented in Fig. 4. On the other hand, the value of K based on Hamaker's microscopic theory indicates a behaviour close to the boundary between Groups B and A particles, hence contradicting the bed-collapse results.

CONCLUSIONS

An experimental study of nanoparticle fluidization is presented. Nanoparticles exhibit homogeneous fluidization, which is a characteristic Group A behaviour, but show typical Group C behaviour at other times (e.g., during initialization of fluidization and bed-collapse tests). We still do not fully understand how this happens, but it seems to be related to the formation of aggregates. For the conditions applied, an overpressure between 10 and 20% was found to be required for incipient fluidization to occur. Analysis shows that both the pressure overshoot and Lifshitz's macroscopic theory give realistic values for the inter-aggregate cohesion force.

ACKNOWLEDGMENT

NOTATION

A_{mi}	Hamaker constant (microscopic theory)
A_{ma}	Hamaker constant (macroscopic theory)
d_a	aggregate diameter
d_{asp}	diameter of asperity
F	cohesion force
F_g	buoyant weight of a single aggregate
H	hardness of the bodies in contact
k	coordination number
K	ratio of cohesion force to single-aggregate buoyant weight
r	geometric mean of the radii of asperities in contact
r_1, r_2	radii of the adhering asperities
R	geometric mean of the radii of agglomerates in contact
R_1, R_2	radii of the adhering agglomerates
Z_0	the distance where the Van der Waals force is maximum
ρ_a	aggregate density
ρ_g	gas density
ε	voidage around the agglomerates
σ	tensile stress

hϖ Lifshitz-Van der Waals constant

REFERENCES

1. Hakim, L.F., Portman, J.L., Casper, M.D., Weimer, A.W. (2005), Aggregation behaviour of nanoparticles in fluidized beds. Powder Technology, **160**, 149-160.

2. Nam, C.H., Pfeffer, R., Dave, R.N., Sundaresan, S. (2004), Aerated vibrofluidization of silica nanoparticles, AIChE J., **50**, 1776-1785.

3. Valverde, J.M., Castellanos, A. (2006), Fluidization of nanoparticles: a modified Richardson-Zaki law, AIChE J., **52**, 838-842.

4. Zhu, C., Yu, Q., Dave, R.N., Pfeffer, R. (2005), Gas fluidization characteristics of nanoparticle agglomerates, AIChE J., **51**, 426-439.

5. Geldart, D. (1973), Types of gas fluidization, Powder Technology, **7**, 285.

6. Geldart, D., Harnby, N., Wong, A.C. (1984), Powder Technology, **37**, 25-37.

7. Wang, X.S., Palero, V., Soria, J., Rhodes, M.J., (2006), Laser based planer imaging of nano-particle fluidization: Part I - determination of aggregate size and shape, Chemical Engineering Science, **61**, 5476-5486.

8. Wang, X.S., Palero, V., Soria, J., Rhodes, M.J., (2006), Laser based planer imaging of nano-particle fluidization: Part II – Mechanistic analysis of nanoparticle aggregation, Chemical Engineering Science, **61**, 8040-8049.

9. Krupp, H. (1967), Particle Adhesion: Theory and Experiment, Adv. Colloid Interface Sci. **1** 111-239.

10. Rumpf, H. Particle Technology, Carl Hanser Verlag, Germany, 1975.

11. Molerus, O. (1975), Theory of Yield of Cohesive Powders, Powder Technology, **12**, 259-275.

12. Visser, J. (1972), On Hamaker Constants: A Comparison between Hamaker Constants and Lifshitz- Van der Waals Constants, Adv. Colloid Interface Sci. **3**, 331-363.

13. Valverde, J.M., Ramos, A., Perez, Castellanos, A., Watson, P.K. (1998), The tensile strength of cohesive powders and its relationship to consolidation, free volume and cohesivity, Powder technology, **97**, 237-245.

14. Jaraiz, E., Kimura, S., Levenspiel, O. (1992), Vibrating beds of fine particles: estimation of interparticle forces from expansion and pressure drop experiments, Powder Technology, **72**, 23-30.

15. Rhodes, M.J., Wang, X.S., Forsyth, A.J., Gan, K.S., Phadtajaphan, S. (2001), Use of magnetic fluidized bed in studying Geldart Group B to A transition, Chemical Engineering Science, **56**, 5429-5436.

16. Rhodes, M.J., Wang, X.S., Nguyen, M., Stewart, P., Liffman, K. (2001), Onset of cohesive behaviour in gas fluidized beds: a numerical study using DEM simulation, Chemical Engineering Science, **56**, 4433-4438.